ACS OMEGA

http://pubs.acs.org/journal/acsodf

Article

Nicotinamide *N*-Methyltransferase Remodeled Cell Metabolism and Aggravated Proinflammatory Responses by Activating STAT3/IL1β/PGE_2 Pathway

Changmei Yang,[#] Tianxiang Wang,[#] Songbiao Zhu, Zhaoyun Zong, Chengting Luo, Yujiao Zhao, Jing Liu, Ting Li, Xiaohui Liu, Chongdong Liu,* and Haiteng Deng*

Cite This: *ACS Omega* 2022, 7, 37509−37519

Read Online

ACCESS | Metrics & More | Article Recommendations | Supporting Information

ABSTRACT: Nicotinamide *N*-methyltransferase (NNMT) is a cytosolic methyltransferase, catalyzing *N*-methylation of nicotinamide (NAM) to form 1-methylnicotinamide (1-MNAM), in which S-adenosyl-L-methionine (SAM) is the methyl donor. It has been well documented that NNMT is elevated in multiple cancers and promotes tumor aggressiveness. In the present study, we investigated the effects of NNMT overexpression on cellular metabolism and proinflammatory responses. We found that NNMT overexpression reduced NAD^+ and SAM levels, and activated the STAT3 signaling pathway. Consequently, STAT3 activation upregulated interleukin 1β (IL1β) and cyclooxygenase-2 (COX2), leading to prostaglandin E2 (PGE_2) accumulation. On the other hand, NNMT downregulated 15-hydroxyprostaglandin dehydrogenase (15-PGDH) which catalyzes PGE_2 into inactive molecules. Moreover, secretomic data indicated that NNMT promoted secretion of collagens, pro-inflammatory cytokines, and extracellular matrix proteins, confirming NNMT aggravated inflammatory responses to promote cell growth, migration, epithelial-mesenchymal transition (EMT), and chemoresistance. Taken together, we showed that NNMT played a pro-inflammatory role in cancer cells by activating the STAT3/IL1β/PGE_2 axis and proposed that NNMT was a potential therapeutic target for cancer treatment.

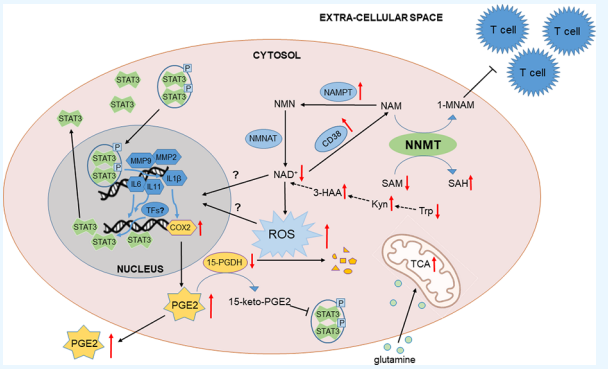

1. INTRODUCTION

Nicotinamide *N*-methyltransferase (NNMT) is a S-adenosyl-L-methionine (SAM)-dependent intracellular enzyme which takes SAM as the methyl donor and catalyzes *N*-methylation of nicotinamide (NAM) to generate 1-methylnicotinamide (1-MNAM) and S-adenosyl-L-homocysteine (SAH). Growing evidence demonstrated that NNMT levels were upregulated in lung adenocarcinoma, kidney renal clear cell carcinoma, pancreatic adenocarcinoma, glioblastoma multiforme, oral squamous cell carcinoma, gastric cancer, ovarian cancer, and in cancer-associated fibroblasts (CAFs) of high-grade serous carcinoma (HGSC).[1−7] According to the data from International Agency for Research on Cancer (IARC), lung cancer has been the leading cause of tumor-related deaths in the world and accounts for 11.4% of the total newly diagnosed cancer cases in 2020.[8] Lung adenocarcinoma is the most common subtype and the only subtype nonsmokers develop.[9,10] NNMT is not only elevated in lung adenocarcinoma tissues compared to adjacent normal tissues, but it is also increased in the serum of nonsmall cell lung cancer (NSCLC) patients.[11,12] In addition, it was reported that NNMT mRNA and protein levels were elevated in gefitinib-resistant NSCLC tissues and cell lines.[13] By contrast, the downregulation of NNMT significantly reduced *in vitro* tumorigenicity of A549 cells.[7] Cancer stem cells in bladder cancer (T24), lung cancer (A549), colorectal cancer (CaCo-2), and osteosarcoma (MG63) cell lines were associated with high NNMT expression.[14] However, the precise mechanisms underlying NNMT-promoted tumor progression remain elusive.

As a substrate of NNMT, NAM is one of the most abundant molecules in cells and one of the precursors for synthesizing NAD^+.[15,16] It was reported that NNMT knockdown significantly increased intracellular NAD^+ levels in mouse adipocytes and HT-29 cells, whereas NNMT overexpression in SW480 cells led to a 30% decrease in NAD^+ levels.[17,18] Our recent studies showed that NAD^+ decline promoted epithelial-mesenchymal transition (EMT) by activating STAT3 signaling pathway and degrading 15-hydroxyprostaglandin dehydrogen-

Received: July 7, 2022
Accepted: October 3, 2022
Published: October 12, 2022

ase (15-PGDH).[19,20] Further, 15-PGDH degradation led to prostaglandin E_2 (PGE_2) accumulation and excretion to tumor microenvironment, resulting in aggravating inflammation. However, it remains to be elucidated whether NNMT can promote EMT and PGE_2 production in cancer cells by depleting NAD^+.

SAM is the other substrate of NNMT, which is the methyl donor for histone and DNA methylation, and for polyamine biosynthesis. It has been reported that NNMT overexpression in 769P cells resulted in a decrease in overall histone H3 methylation, while silencing NNMT in SKOV3 cells resulted in an increase in overall histone H3 methylation.[21] However, little is known about how NNMT regulates gene expression through consuming SAM and NAM. In the present study, we investigated the effects of NNMT overexpression on cellular metabolism and inflammatory response. The results showed that NNMT promoted secretion of collagens, pro-inflammatory cytokines, and extracellular matrix proteins to enhance proinflammatory responses, which drove cell growth, migration, epithelial-mesenchymal transition (EMT), and chemoresistance. All these data suggested that NNMT aggravated inflammation in cancer cells and is a potential therapeutic target in cancer treatment.

2. MATERIALS AND METHODS

2.1. Cell Culture. A549 cells (purchased from the cell bank of the Chinese Academy of Sciences) were cultured in RPMI-1640 medium (Wisent, Montreal, Canada). The culture medium was supplemented with 10% fetal bovine serum (FBS) (PAN-Biotech, Germany) and 1% penicillin/streptomycin (Wisent, Montreal, Canada). 293T cells were cultured in DMEM medium with 10% FBS and 1% penicillin/streptomycin. Cells were cultured in an incubator.

2.2. Establishment of a Stable NNMT-Overexpressing Cell Line. Human NNMT cDNA was obtained from HepG2 cell line. A Flag tag was added at the C-terminus and NNMT cDNA was then cloned into PLVX-IRES-ZsGreen1 lentiviral transfer vector. The 293T cell line was transfected with PLVX-IRES-ZsGreen1 or PLVX-NNMT-IRES-ZsGreen1 using lentiviral packaging vectors and polyethylenimine (Sigma, St Louis, MO, USA). Supernatants were harvested after 72 h and concentrated with PEG6000. Precipitated lentiviral particles were resuspended in phosphate buffered saline (PBS). A549 cells were infected in the presence of 5 μg/mL Polybrene (Sigma, St Louis, MO, USA). Infected cells (Ctrl and NNMT-OE cells) with green fluorescence were sorted by flow cytometry and used for further analysis.

2.3. Establishment of Stable IL1β-Knockdown Cell Line. The shRNA-containing plasmids (pLKO.1) for IL1β knockdown were purchased from the shared instrument facility at the Center for Biomedical Analysis of Tsinghua University. The shRNA-containing plasmids were cotransfected with pLP2, pLP/VSVG, and pLP1 into 293T cells by polyethylenimine. After 72 h, cell culture supernatants were collected and concentrated using PEG6000. The lentiviral particles were resuspended using PBS. NNMT-OE cells were transfected with lentiviral particles for 10 h in the presence of 5 μg/mL Polybrene. Cells were selected in the presence of 2 μg/mL puromycin to obtain stable knockdown cell lines, which were then verified by qPCR and Western blotting.

2.4. Quantitative Real-Time PCR (qPCR). Total RNA was isolated from cells with Trizol reagent (TIANGEN, Beijing, China). cDNA was synthesized from 2 μg total RNA by using the reverse transcription kit (CWBIO, Beijing, China) according to the manufacturer's instructions. qPCR was performed with the Roche LightCycler 96 System (Roche, Basel, Switzerland) by using an SYBR green reaction mixture (CWBIO, Beijing, China). β-Actin was used as the internal control for relative quantification. Primers used in qPCR are listed in Supplementary Table 1.

2.5. Western Blotting Analysis. Cells were lysed in RIPA lysis buffer (Beyotime, Beijing, China) added with a Protease inhibitors cocktail. Equal volumes of proteins were separated on 12% SDS-PAGE gel and electro-transferred onto a polyvinylidence difluoride (PVDF) membrane. Primary anti-NNMT, anti-ZO-1, anti-Snail, anti-Cytokeratin-18, anti-Stat3, anti-Stat3 pS727, anti-Stat3 AcK685, anti-TGFβ2 (Proteintech, Rosemont, USA), anti-HPGD (Bioworld), anti-COX2, anti-E-cadherin, anti-N-cadherin (Cell Signaling Technology), and secondary antirabbit HRP-IgG antibodies (CST, Danvers, MA) were used for immunoblotting.

2.6. Cell Proliferation Assay with Cell Counting Kit-8 (CCK-8). Equal numbers of cells were seeded and cultured in 96-well plates. The cell proliferation rate was determined with CCK-8 (Dojindo, Kumamoto, Japan) reagent. The plates were incubated in a cell incubator containing 5% CO_2 at 37 °C for 2 h. Then the absorbance at 450 nm was measured.

2.7. Susceptibility of Ctrl and NNMT-OE A549 Cells to Cisplatin. Ctrl and NNMT-OE A549 cells were seeded into 96-well plates with 4000 cells/well. After 48 h of incubation, cells were treated with cisplatin (Selleck, Houston, TX) in five replicates for 24 h. CCK-8 reagent was added to treated cells and incubated at 37 °C for 2 h. Then the absorbance at 450 nm was measured. Cell viability was represented as the percentage of viable cells compared to untreated cells.

2.8. Colony Formation Assay. Cells were seeded in a 6-well plate at 1000 cells/well. A549 Ctrl and NNMT-OE cells were cultured at 37 °C. The colonies were fixed with 1 mL of 4% paraformaldehyde solution for 15 min at room temperature. The colonies were then rinsed with PBS. A 500 μL aliquot of 1% crystal violet staining solution (Solarbio, Beijing, China) was added into each well and incubated for 30 min at room temperature. Excessive crystal violet staining solution was removed, and the colonies were imaged by using the Image Lab software (Bio-Rad Laboratories, CA, USA).

2.9. Sample Preparation for Quantitative Proteomic Analysis. Proteomic analysis was performed as described previously.[20] Briefly, a total of 100 μg of protein was extracted from cells with 8 M urea containing a 1% protease inhibitors cocktail. Then, the proteins were digested with trypsin at 37 °C overnight. Tryptic peptides were desalted and labeled with the TMT 6-plex reagent. Then, the mixed labeled peptides were subjected to liquid chromatography-tandem mass spectrometry (LC-MS/MS) analysis.

2.10. Sample Preparation for Secretomic Analysis. Secretomic analysis was performed as described previously.[20] Briefly, cells were cultured in medium supplemented with 10% FBS until they reached 70% confluency. Then cells were washed with PBS three times and further incubated in serum and phenol red-free medium at 37 °C for 24 h. Medium was collected and centrifuged at 10,000 rpm for 10 min to remove large debris. Supernatants were collected, and five volumes of ice-cold acetone added, followed by overnight precipitation at −20 °C. The pellets were dissolved in 8 M urea, and protein concentration was determined using a BCA protein assay kit (Solarbio, Beijing, China). Equal protein amounts were used

https://doi.org/10.1021/acsomega.2c04286
ACS Omega 2022, 7, 37509−37519

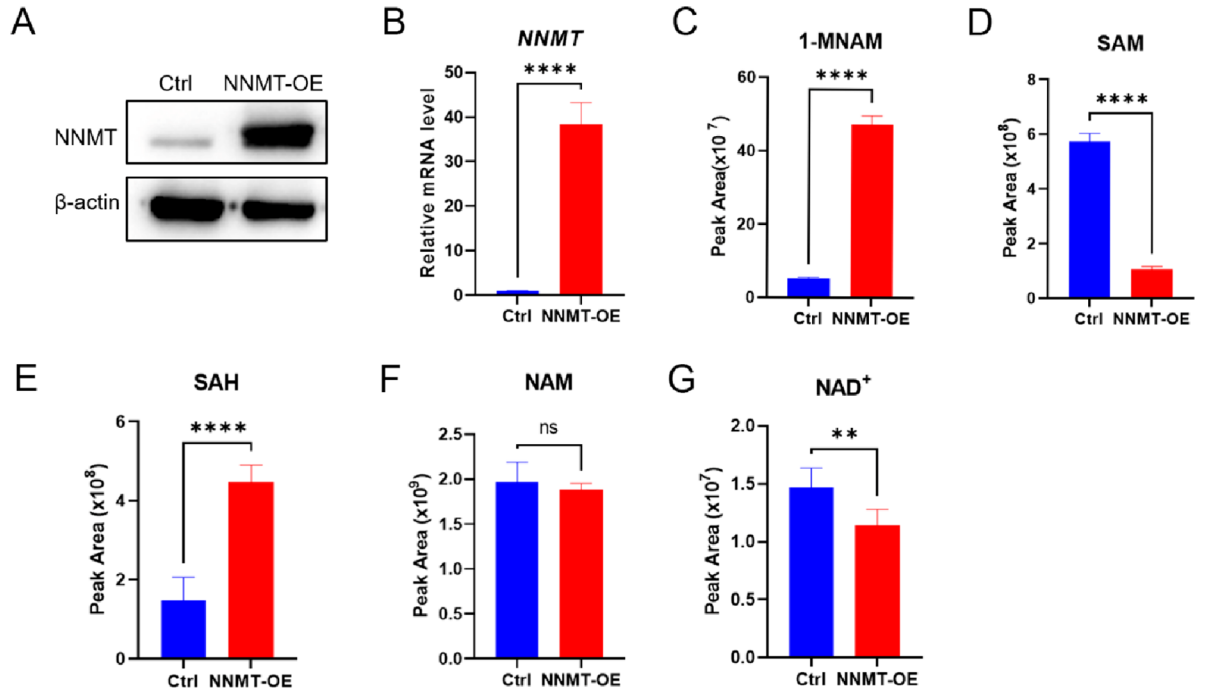

Figure 1. NNMT remodeled cell metabolism and reduced NAD^+ levels. (A) Western blotting analysis confirmed NNMT overexpression in A549 cells. (B) QPCR analysis confirmed NNMT overexpression in A549 cells. (C) Targeted metabolomics data showed that NNMT overexpression resulted in 1-MNAM accumulation by almost 9-fold (n = 5). (D) SAM was significantly reduced in NNMT-OE cells (n = 5). (E) SAH was markedly elevated in NNMT-OE cells (n = 5). (F) NAM levels were not altered after NNMT overexpression (n = 5). (G) NAD^+ levels declined in NNMT-OE cells by using targeted metabolomics (n = 5). Data were analyzed using Student's t test. ****p < 0.0001. ***p < 0.001. **p < 0.01. *p < 0.05 was considered statistically significant. All values represent mean from at least three biological replicates ± SD.

for the following experiment the same as quantitative proteomic analysis.

2.11. LC-MS/MS Analysis. Labeled peptides were injected on an Ultimate 3000 HPLC system that was directly interfaced with a Thermo Orbitrap Fusion Lumos mass spectrometer and separated by a 120 min gradient elution with a flow rate of 0.300 μL/min. The analytical column was a C-18 (300 Å, 5 μm, Thermo Fisher Scientific, USA) resin packed fused silica capillary column (75 μm inner-diameter, 150 mm length, Thermo Fisher Scientific, USA). Mobile phase A consisted of 0.1% formic acid, and mobile phase B consisted of 100% acetonitrile and 0.1% formic acid. The mass spectrometer was operated in the data-dependent acquisition (DDA) mode using Xcalibur 4.1.31.9 software, and MS1 spectra were acquired at a mass range of 300−1800 m/z with a resolution of 60,000. The spray voltage was 3800 V, and the Automatic Gain Control (AGC) target was $3e^6$. For MS2 scans, the top 20 most intense precursor ions were fragmented in the HCD collision cell at a normalized collision energy of 32% using a 0.7 Da isolation window, and the dynamic exclusion duration was 15 s. The AGC target was $1e^5$ whereas the maximum injection time was 100 ms.

2.12. Protein Identification and Quantification. The raw mass spectrometry data were searched against the *Homo sapiens* database by the Proteome Discoverer 2.3 software. The following parameters were used for database searching: static modifications of TMT 6-plex on lysine or peptide N terminus (+229.13 Da) and carbamidomethylation (+57.021 Da) on cysteine; dynamic modification of oxidation (+15.995 Da) on methionine; two missed cleavages were allowed; the mass tolerances of precursors and fragments were 10 ppm and 0.02 Da, respectively; at least one unique peptide for quantification of proteins; only peptides with false discovery rate (FDR) below 1% were considered as high-confidence hits.

2.13. Metabolomics. Cold methanol extraction was used for the collection of cell metabolic products.[22] Briefly, the cells were washed twice with ice cold PBS and were extracted using prechilled 80% methanol (−80 °C). Macromolecules and debris were removed by centrifugation, and the metabolites within the supernatant were concentrated by drying completely using a Speedvac for mass spectroscopy analysis. The chromatographic peak area was used to represent the relative abundance of a metabolite, and the protein content was used for normalization.

2.14. Detection of Cellular Reactive Oxygen Species (ROS). The cellular reactive oxygen species were detected by using CellROX Deep Red Reagents (Invitrogen, NY, USA). Briefly, cells were washed twice with PBS and stained with 5 μM CellROX Deep Red reagent. After staining for 30 min at 37 °C, the fluorescence of 20,000 cells was analyzed by using a BD Flow Cytometer (BD Biosciences, NJ, USA). Relative quantification was determined by the mean emission fluorescence intensity at 665 nm.

2.15. Wound Healing Assay. A wound healing assay was performed according to the method described in our previous study.[23] Briefly, monolayer cells with 95% confluence were wounded by scratching the surface of each well in a 6-well plate as uniformly as possible with a 200 μL pipet tip. The wells were then rinsed with PBS three times, and the well was replenished with 1640 medium without FBS, incubated at 37 °C for 72 h. Images of the initial wound, and the movement of cells into the scratched area, were captured using a Nikon microscope (Olympus Corporation, Tokyo, Japan) at 0 and 72 h. This assay was done in triplicates.

https://doi.org/10.1021/acsomega.2c04286
ACS Omega 2022, 7, 37509−37519

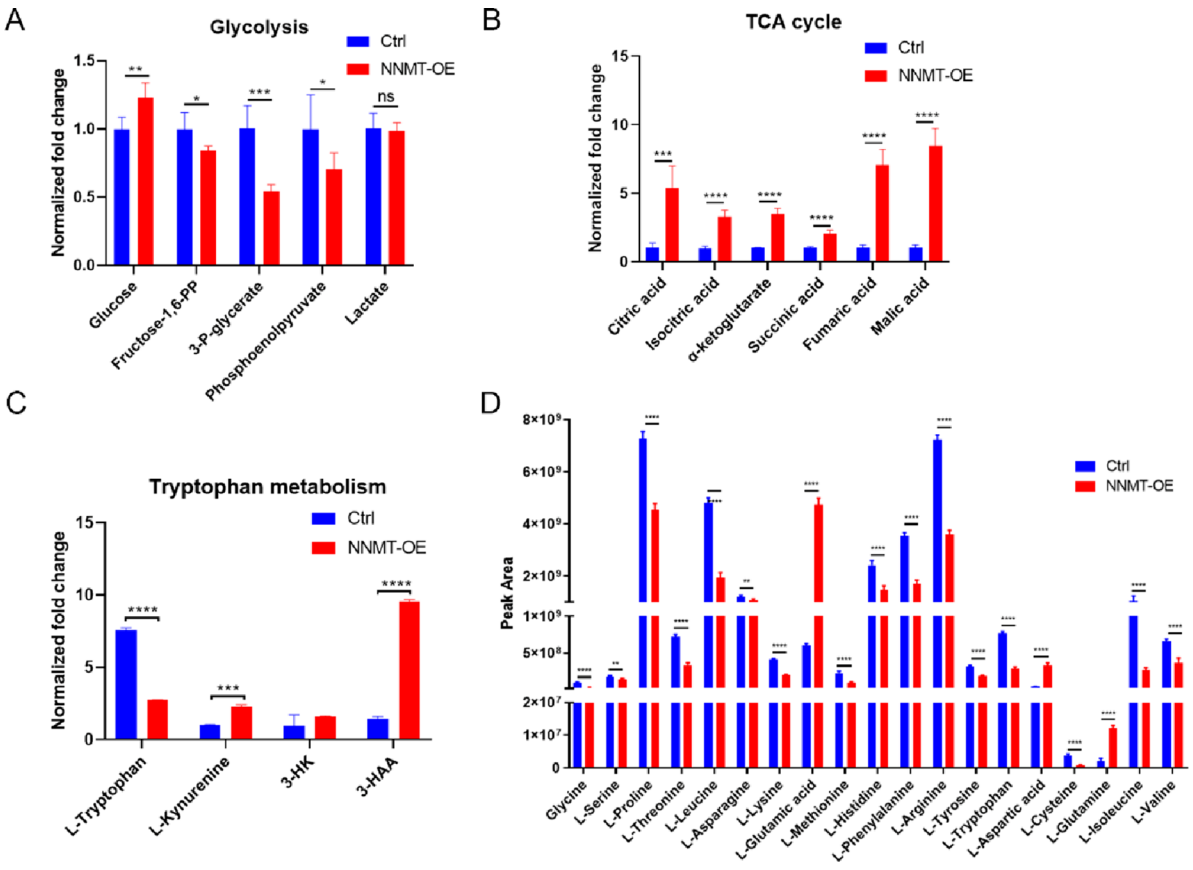

Figure 2. NNMT affected multiple metabolic pathways. (A) Intermediates in glycolysis pathway were found downregulated by untargeted metabolomics, suggesting NNMT caused glycolysis inhibition which was confirmed by the subsequent proteomic data (n = 5). (B) Intermediates in TCA cycle markedly accumulated in NNMT-OE cells which was confirmed by the subsequent proteomic data (n = 5). (C) Metabolites in tryptophan metabolism, among them kynurenine increased by 2-fold and 3-HAA increased by 6-fold (n = 4). (D) Most of amino acids were downregulated in NNMT-OE cells except for aspartic acid, glutamic acid and glutamine (n = 5). Data were analyzed using Student's t test. ****p < 0.0001. ***p < 0.001. **p < 0.01. *p < 0.05 was considered statistically significant. All values represent mean from at least three biological replicates ± SD. Fructose-1,6-PP, Fructose-1,6-bisphosphate. 3-P-glycerate, 3-phosphoglycerate. 3-HK, 3-hydroxykynurenine. 3-HAA, 3-hydroxyanthranilic acid.

2.16. Lung Adenocarcinoma Xenografts in Nude Mice. A mice experiment was performed in the animal facility of Tsinghua University (Beijing, China) with approval of the Institutional Animal Care and Use Committee of Tsinghua University. A total of 10 male nude mice (6 weeks old, 20−22 g) were purchased from an external source with a health certificate (Sterling, China) and were housed under specific pathogen-free conditions at Laboratory Animal Research Center, Tsinghua University. A549 Ctrl and NNMT-OE cells (2×10^6 cells) in 200 μL of prechilled PBS were subcutaneously injected into the right underarm of mice. Tumor growth was measured every other day using a digital caliper. All mice were sacrificed 35 days after injection, and the tumors were harvested, washed, and photoed.

2.17. Statistical Analysis. R (version 4.3) and GraphPad Prism software (version 9.0) were used for statistical analysis and plotting. Student's t test and one-way ANOVA test were used to determine the significance of differences, and p-values less than 0.05 were considered to be significant.

3. RESULTS

3.1. NNMT Remodeled Cell Metabolism and Decreased NAD$^+$ Levels. To investigate the effects of NNMT on cell metabolism, we stably constructed a cell line by overexpressing NNMT in A549 cells using an established protocol.[24] NNMT-overexpressing (NNMT-OE) A549 cells were confirmed by Western blotting and qPCR (Figure 1A, 1B). NAM is the precursor for NAD$^+$ synthesis from the salvage pathway. To examine NNMT activity, we detected NAM, 1-MNAM, SAM, and SAH levels by using targeted metabolomics. As expected, 1-MNAM was 9-fold higher in NNMT-OE cells than that in control (Ctrl) cells, confirming that NNMT was successfully overexpressed in A549 cells with enzyme activity (Figure 1C). Additionally, SAM levels decreased dramatically while SAH levels increased by 2-fold in NNMT-OE cells when compared with Ctrl cells (Figure 1D, 1E). Unexpectedly, NAM was not altered by NNMT overexpression (Figure 1F). Given that NAM was not changed, we measured NAD$^+$ levels by targeted metabolomics and found NAD$^+$ levels reduced by approximately 25% (Figure 1G), suggesting that the breakdown of NAD$^+$ was responsible for the unchanged NAM levels.

In addition to metabolites closely related to NNMT functions, we also analyzed other metabolites in NNMT-OE cells by using untargeted metabolomics. As Figure 2A shows, glucose was elevated in NNMT-OE cells while the intermediates in glycolysis such as fructose-1,6-PP, 3-P-glycerate, and phosphoenolpyruvate were reduced and lactate was not altered, indicating that glycolysis may be suppressed.

https://doi.org/10.1021/acsomega.2c04286
ACS Omega 2022, 7, 37509−37519

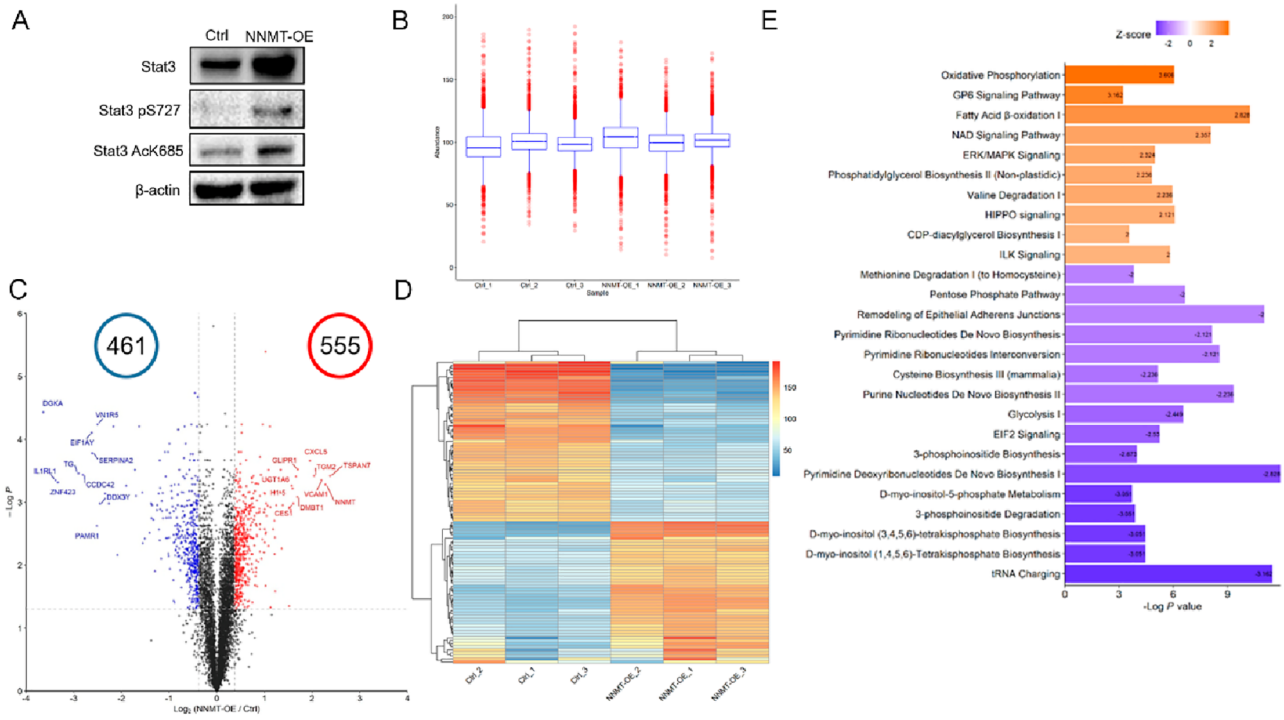

Figure 3. NNMT activated STAT3 and proteomic analysis was performed for Ctrl and NNMT-OE cells. (A) Western blotting analysis for STAT3, STAT3 AcK685, STAT3 pS727, and β-actin expression levels in Ctrl and NNMT-OE cells. (B) Abundance distribution of proteins from all the biological replicates. (C) Volcano plots revealed significantly changed proteins between Ctrl and NNMT-OE cells, in which blue dots in upper left and upper right sections represent proteins with fold-change <0.77 or >1.3 and p values <0.05 from t test statistics. (D) Heatmap clustering analysis showed hierarchical patterns and differentially expressed proteins (top 100) in Ctrl and NNMT-OE A549 cells. (E) IPA analysis for those differentially expressed proteins.

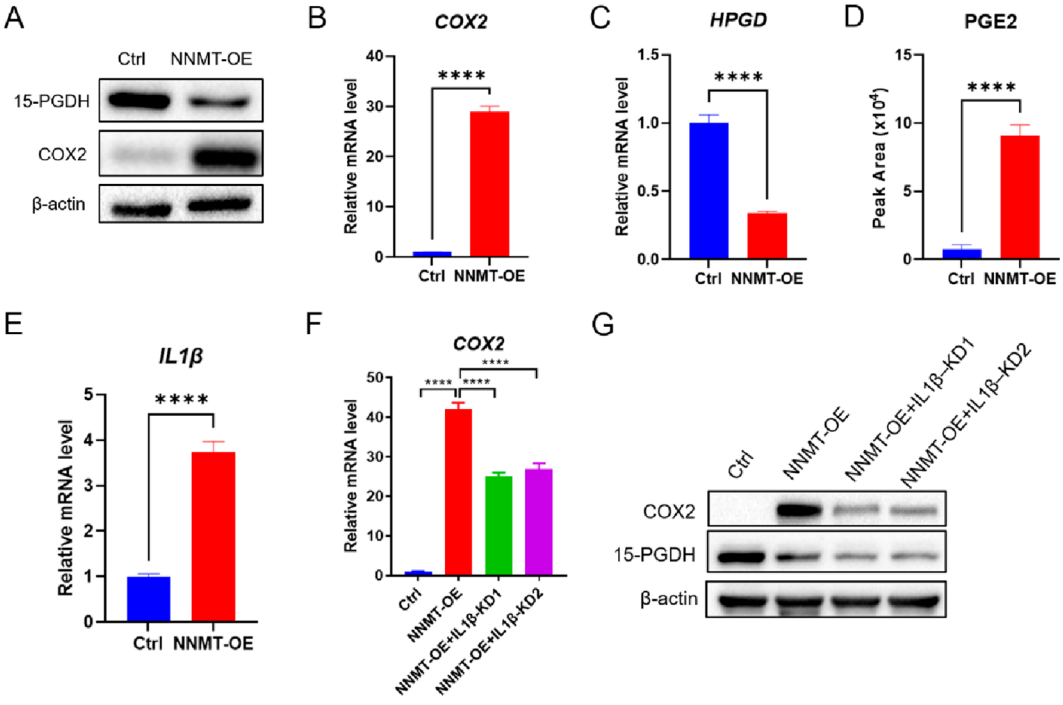

Figure 4. NNMT promoted IL1β-induced COX2 expression and downregulated 15-PGDH. (A) Western blotting analysis for COX2 and 15-PGDH in Ctrl and NNMT-OE cells. (B) qPCR analysis for the mRNA levels of *COX2*. (C) qPCR analysis for the mRNA levels of *HPGD*, the gene coding 15-PGDH. (D) Targeted metabolomics data showed that PGE_2 accumulated in NNMT-OE cells by almost 10-fold (n = 4). (E) NNMT promoted the production of IL1β in large quantity. (F) IL1β knockdown in NNMT-OE cells led to reduced expression of COX2 mRNA levels. (G) Western blotting analysis confirmed that IL1β knockdown in NNMT-OE cells led to reduced COX2 protein levels. Data were analyzed using Student's t test or one-way ANOVA test. ****p < 0.0001. ***p < 0.001. **p < 0.01. *p < 0.05 was considered statistically significant. All values represent mean from at least three biological replicates ± SD.

https://doi.org/10.1021/acsomega.2c04286
ACS Omega 2022, 7, 37509−37519

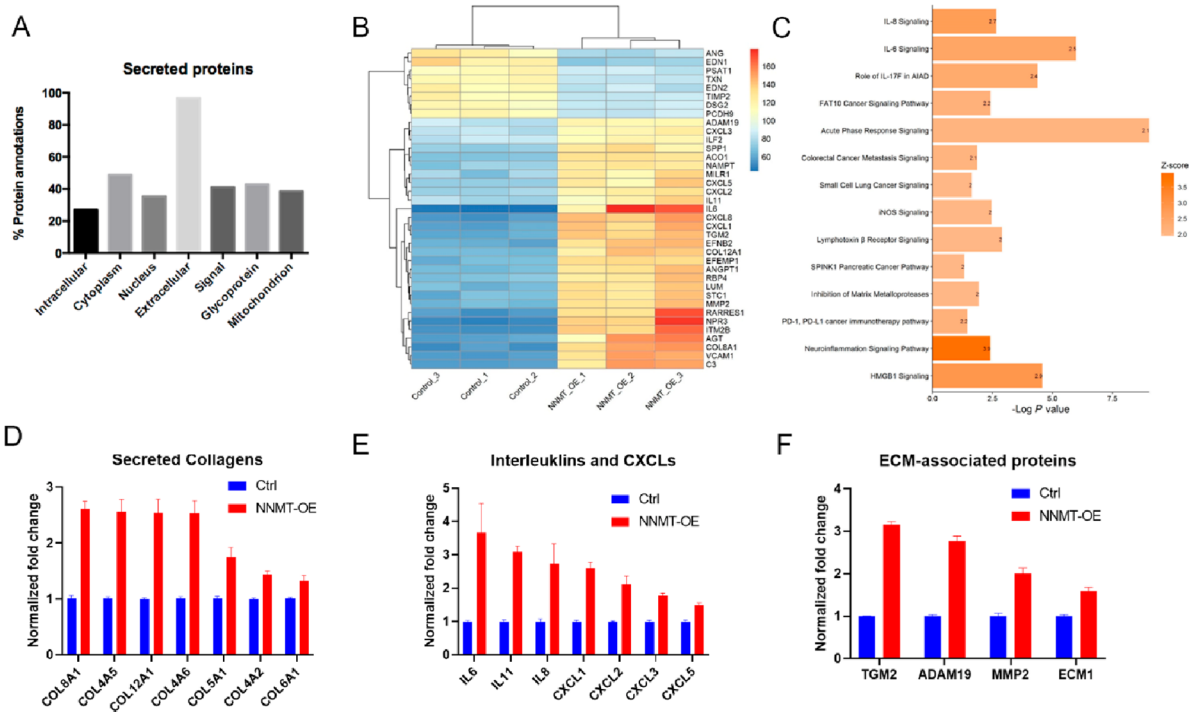

Figure 5. Secretomic analysis showed that NNMT-OE cells secreted abundant pro-inflammatory cytokines, collagens, and ECM proteins. (A) Categorization of identified proteins after bioinformatics analysis. Uniprot proteome database with the keywords "Signal" and "Extracellular" were used to filter identified proteins. (B) Heatmap displayed 39 significantly changed secreted proteins including IL-6, IL-11 etc. (C) IPA analysis for secreted proteins which were significantly changed. (D–F) Normalized fold change of secreted collagens, interleukins, and CXCLs as well as ECM-associated proteins from secretomic data.

Moreover, metabolites in TCA cycle were significantly accumulated (Figure 2B), implying that NNMT promoted oxidative phosphorylation in cancer cells. Downregulation of proteins associated with glycolysis and upregulation of proteins in oxidative phosphorylation were confirmed by the subsequent proteomic analysis. Interestingly, we found tryptophan was markedly decreased accompanied by increased kynurenine and 3-hydroxyanthranilic acid (3-HAA) (Figure 2C). Specifically, kynurenine was increased by 2-fold while 3-HAA was increased by 6-fold. NNMT-overexpression also led to the lower levels of amino acids except for glutamic acid, glutamine, and aspartic acid (Figure 2D). Taken together, NNMT reduced NAD^+ levels and remodeled cell metabolism in cancer cells with enhanced oxidative phosphorylation.

3.2. NNMT Decreased 15-PGDH and Activated STAT3/IL1β/PGE_2 Pathway. Our previous studies indicated that NAD^+ decline activated the STAT3 signaling pathway and drove the EMT process.[20] Similarly, NNMT overexpression also reduced NAD^+ levels and activated STAT3 by upregulating STAT3 and promoting S727 phosphorylation and K685 acetylation of STAT3 (Figure 3A), which were crucial in the activation of STAT3 and regulated cancer-associated inflammation.[25−29] To comprehensively investigate the underlying mechanisms of NNMT in cancer-associated inflammation, proteomic analysis was performed by using Ctrl and NNMT-OE cells. Experiments were conducted in biological triplicates, with a total of 8115 proteins identified and 6502 proteins identified in all three replicates (Supplementary Table 2). Figure 3B is the abundance boxplot of each sample labeled with TMT. Based on fold change (>1.3 or <0.77) and p values ($p < 0.05$), 1016 proteins were considered as differentially expressed proteins (DEPs) between Ctrl and NNMT-OE cells, in which 461 proteins were down-regulated and 555 were up-regulated (Supplementary Table 3). Blue and red dots in the volcano plot indicate the downregulated and upregulated proteins with a significant difference, respectively (Figure 3C). Heatmap clustering analysis showed hierarchical patterns and correlations of differentially expressed proteins in Ctrl and NNMT-OE cells (Figure 3D). Furthermore, Ingenuity pathway analysis (IPA) was conducted to analyze these DEPs, and the results strongly suggested that NNMT activated oxidative phosphorylation, fatty acid β-oxidation, NAD signaling pathway, ERK/MAPK signaling, and ILK signaling which resulted in phosphorylation of AKT, GSK-3, and other signaling proteins that regulated gene expression for cell proliferation[30] (Figure 3E). Conversely, NNMT inhibited the pentose phosphate pathway, glycolysis, remodeling of epithelial adherens junctions, EIF2 signaling, and tRNA charging (Figure 3E). Consistent with metabolic analysis, the proteomic data supported that NNMT attenuated glycolysis and enhanced oxidative phosphorylation in cancer cells.

Among those DEPs, COX2 was increased by 2.6-fold while 15-PGDH was decreased by 4-fold, respectively (Supplementary Table 3). Then we confirmed elevated COX2 protein levels and reduced 15-PGDH protein levels in NNMT-OE cells by Western blotting and qPCR (Figure 4A–4C). COX2 is an inducible enzyme catalyzing the formation of PGE_2 from arachidonic acid which is normally absent in most tissues, and its expression is induced by a wide range of inflammatory stimuli.[31−33] Inversely, 15-PGDH catalyzes NAD^+-linked oxidation of PGE_2 and is the key enzyme responsible for the biological inactivation of these eicosanoids. Consequently, we found that PGE_2 increased by almost 10-fold in NNMT-OE A549 cells (Figure 4D).

https://doi.org/10.1021/acsomega.2c04286
ACS Omega 2022, 7, 37509−37519

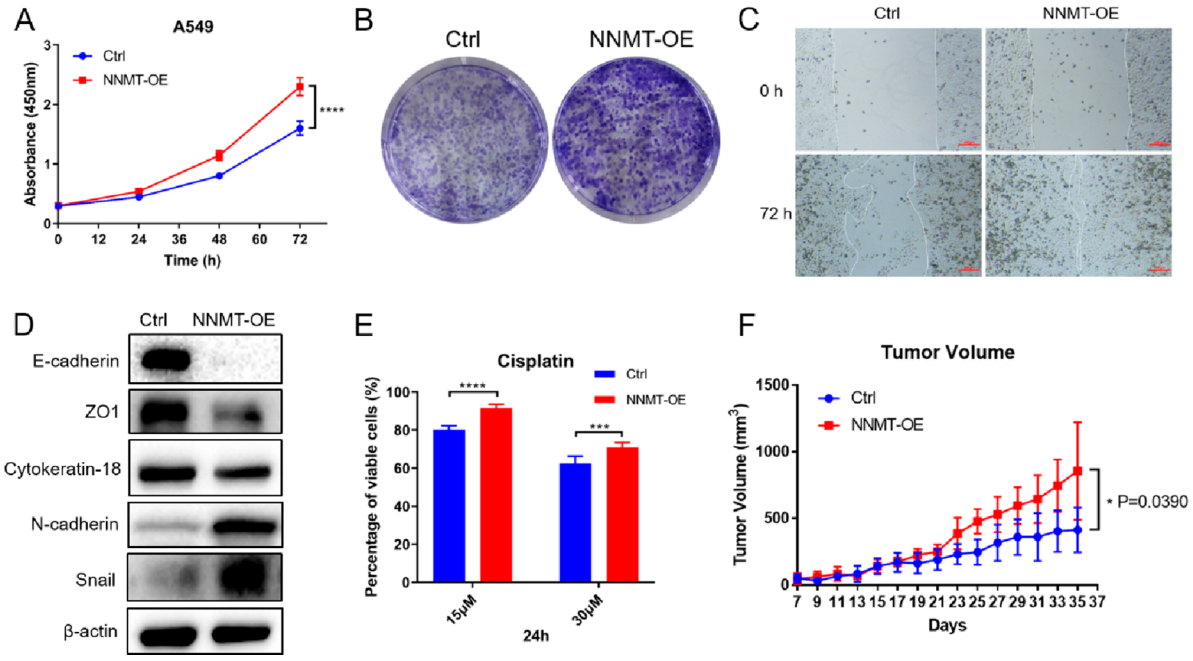

Figure 6. NNMT aggravated the progression of cancer cells. (A) Overexpression of NNMT in A549 increased the growth rate of cells; cell growth was detected using the CCK-8 kit. (B) Representative images of colony forming assay for Ctrl and NNMT-OE cells, indicating that NNM-OE promoted colony forming ability of A549 cells. (C) Cell migration was enhanced in NNMT-OE cells compared with that in control cells, assessed by the wound healing assay. Cells were imaged at 0 hand 72 h after scratching. Scale bar: 200 μm. (D) Western blotting of EMT markers such as ZO-1, Cytokeratin-18, E-cadherin, N-cadherin, Snail, and β-actin expression in Ctrl and NNMT-OE A549 cells. (E) 2×10^6 of Ctrl and NNMT-OE cells were injected into the right underarm of nude mice ($n = 5$). Tumor volume was measured every 2 days. SD is indicated by error bars. *$p <$ 0.05 versus control cells. (F) Percentage of viable cells between Ctrl and NNMT-OE A549 cells treated with different concentration of cisplatin ($n = 5$). Data were analyzed using Student's t test. ****$p < 0.0001$, ***$p < 0.001$, **$p < 0.01$. *$p < 0.05$ was considered statistically significant. All values represent mean from at least three biological replicates ± SD.

COX2 gene expression is usually promoted by pro-inflammatory cytokine IL1β.[33] NNMT overexpression resulted in enhanced IL1β production (Figure 4E). To test whether COX2 was induced by IL1β, we knocked down IL1β gene expression by using shRNA and found that IL1β silencing caused a marked COX2 decline in both mRNA and protein levels (Figure 4F, 4G). Notably, it is known that IL1β, COX2, IL-6, IL-8, IL11, MMP2, and MMP9 are STAT3 target genes.[29] Thus, the upregulation and activation of STAT3 by NNMT promoted IL1β, COX2, and PGE_2 production. In summary, NNMT decreased 15-PGDH, activated the STAT3/IL1β/PGE_2 pathway, and resulted in inflammatory PGE_2 accumulation.

3.3. Secretomic analysis revealed that NNMT promoted the secretion of multiple pro-inflammatory cytokines and extracellular matrix proteins. NNMT overexpression activated the STAT3 signaling pathway and up-regulated DEPs between Ctrl and NNMT-OE A549 cells, which were closely related to extracellular structure and matrix organization. By secretomic analysis, we identified 1396 authentically secretory proteins by searching the Uniprot proteome database annotated for "Signal" and "Extracellular" proteins (Figure 5A, Supplementary Table 4). By using the cutoff fold change values (<0.77 or >1.3) and p values (<0.05), we found that 134 proteins were upregulated while 145 proteins were downregulated (Supplementary Table 5). Heatmap clustering analysis listed the significantly changed proteins such as IL11, IL6, MMP2, VCAM1, TGM2, ADAM19, multiple collagens, and CXCLs in Figure 5B. It is worth noting that IL6 and IL11 are activators for STAT3.[29] Moreover, IPA analysis demonstrated that NNMT over-expression activated various pathways that promoted cancer progression (Figure 5C).

Combined with the proteomic data, we found that intracellular transforming growth factor β2 (TGFβ2) increased by 2-fold while secreted TGFβ2 increased by 1.5-fold (Figure S1A, S1B). Quantitative PCR and Western blotting analysis showed remarkable production of TGFβ2 in NNMT-OE cells (Figure S1C, S1D). It is increasingly recognized that TGFβ2 has strong immunosuppressive properties and regulates key mechanisms of carcinogenesis, metastasis, and chemoresistance.[34] From secretomic data, histograms displayed the enhanced secretion of collagens, extracellular matrix proteins as well as interleukins, chemokines (Figure 5D−5F). We detected some matrix metalloproteinases (MMPs) by qPCR, and the results showed that the mRNA levels of MMP2, MMP3, and MMP9 were significantly upregulated (Figure S1E−S1G). In agreement with the activation of the STAT3 pathway, NNMT promoted the secretion of multiple pro-inflammatory cytokines, extracellular matrix proteins, PGE_2 and TGFβ2, which changed the tumor microenvironment. Together, high NNMT levels changed the secretome atlas of cancer cells and aggravated cancer-associated inflammation.

3.4. NNMT aggravated the progression of cancer cells. STAT3 signaling is a major pathway for inflammation. Cytokines, chemokines, and other mediators like IL6, IL1β, and COX2, are important for inducing and maintaining a cancer-promoting inflammatory environment, and STAT3 is essential for regulating their expressions.[35] The proliferation ability of NNMT-OE cells was measured by growth curve and colony-forming assay, and the results showed that NNMT-OE cells grew faster than Ctrl cells and possessed stronger colony-

https://doi.org/10.1021/acsomega.2c04286
ACS Omega 2022, 7, 37509−37519

forming abilities (Figure 6A, 6B). Wound healing assay indicated that NNMT promoted cancer cell migration (Figure 6C). These data are consistent with a previous observation using the NNMT knockdown A549 cell line,[7] NNMT overexpression significantly promoted cell proliferation, migration, and colony-forming capacity of cancer cells.

Furthermore, we monitored protein levels of EMT markers such as E-cadherin, ZO-1, Cytokeratin-18, N-cadherin, and Snail (Figure 6D). These results suggested that NNMT promoted the EMT process. In terms of cell morphology, NNMT-OE cells became more elongated, similar to the shape of intermediate cells during EMT process (Figure S2A). In addition, to assess the pro-proliferation activity of NNMT *in vivo*, Ctrl and NNMT-OE cells (2×10^6 cells) were subcutaneously injected into mice. Consistent with *in vitro* data, NNMT-OE cells possessed stronger oncogenicity and proliferative ability *in vivo* (Figures 6E, S2B, S2C). A genome-wide analysis identified NNMT as one of eight invasion-related genes and chemo-resistant genes which can be utilized to predict the relapse-free survival time in the lung cancer cohorts.[36] Thus, we measured the chemotherapy sensitivity of NNMT-OE cells after cisplatin treatment for 24 h. It is obvious that NNMT-OE cells were more chemoresistant than Ctrl cells after cisplatin treatment (Figure 6F). NNMT overexpression aggravated the progression of cancer cells by promoting cell proliferation, migration, EMT, colony formation ability, and chemoresistance.

4. DISCUSSION

It has been shown that NNMT mRNA and protein are both highly expressed in various cancers and NNMT is considered as a potential biomarker and therapeutic target.[37,38] A few studies indicated that NNMT was more sensitive than carcinoembryonic antigen (CEA) for diagnosis of lung adenocarcinoma and colorectal cancer (CRC), and combined testing of NNMT and CEA in serum can improve the diagnosis accuracy.[11,12,39,40] The present study explored the underlying mechanisms of NNMT on cell metabolism and inflammatory responses by performing proteomics, secretomics, and metabolomics. Herein, we reported that NNMT overexpression in cancer cells reduced NAD^+ levels and remodeled cell metabolism. Specifically, glycolysis was attenuated while oxidative phosphorylation was enhanced in NNMT-OE cells and NNMT rendered cells more addicted to glutamine. Reliance on glutamine has long been considered to be a hallmark of cancer cell metabolism and this phenomenon is known as glutamine addiction which depicts an increased dependency of cancer cells on other nutrients to feed the TCA cycle.[41,42] Of note, NNMT promoted the accumulation of kynurenine and 3-HAA. The kynurenine pathway (KP) of tryptophan metabolism in cancer cells has emerged as a key metabolic pathway contributing to immune escape. Among the KP metabolites, 3-HAA appears to have the strongest capacity to modulate the immune functions.[43] A recent report showed that compared with the control subjects, the patients with NSCLC exhibited significantly lower levels of tryptophan and significantly higher levels of 3-HAA.[44] Besides, the patients with low 3-HAA had remarkably longer progression free survival (PFS) than those with high 3-HAA.[44] Accordingly, NNMT may promote tumor aggressiveness through activation of tryptophan metabolism and accumulation of KP metabolites.

Intriguingly, intracellular NAM levels were not changed after NNMT overexpression which may be attributed to the quick uptake of NAM from culture medium or the NAD^+ breakdown by Sirtuins, PARPs or CD38. Indeed, CD38 was upregulated by 2-fold in the proteomic data (Supplementary Table 3) which may be a factor affecting NAD^+ levels in NNMT-OE cells. Our previous paper showed that CD38 overexpression caused 15-PGDH degradation[19] and the EMT process which was consistent with the current findings. COX2 was induced by IL1β which is a target gene of STAT3. The reciprocal regulation of COX2 and 15-PGDH was reported in lung adenocarcinoma before.[45] However, this is the first report that COX2 and 15-PGDH were inversely regulated by NNMT in lung adenocarcinoma cells. Moreover, it was reported that the COX2/PGE_2 signaling pathway induced EMT and COX2 can potentiate cisplatin resistance in lung cancer cells.[46,47]

Given that NNMT overexpression activated the pro-inflammatory response, we carried out secretomic analysis and found NNMT promoted the secretion of various pro-inflammatory cytokines, collagens, chemokines, and ECM-related proteins. All these results supported the conclusion that NNMT promoted tumor progression and NNMT secreted pro-inflammatory factors like PGE_2, interleukins, and MMPs to promote progression of cancer cells, suggesting that NNMT is a potential therapeutic target. However, how NNMT affected the expression of STAT3 is unresolved. NNMT may alter SAM levels, leading to histone or DNA hypomethylation. In addition, it is unknown which genes will be altered in their expression when SAM levels are reduced by NNMT. It is worth exploring how NNMT-OE cells interplay with immune cells or stromal cells in tumor microenvironment by secreting 1-MNAM, IL1β, IL6, IL11, and TGFβ2.

In conclusion, our multiomic analysis demonstrated that NNMT aggravated tumor inflammatory responses and promoted cancer progression via the STAT3/IL-1β/PGE_2 pathway, and NNMT remodeled cell metabolism with enhanced oxidative phosphorylation and tryptophan metabolism. These results indicate that NNMT is a potential therapeutic target for cancer treatment.

■ ASSOCIATED CONTENT

Supporting Information

The Supporting Information is available free of charge at https://pubs.acs.org/doi/10.1021/acsomega.2c04286.

Supplementary tables (ZIP)

NNMT promoted the expression and secretion of TGFβ2 as well as some MMPs; NNMT overexpression changed cell morphology and promoted cancer cell growth in vivo (PDF)

■ AUTHOR INFORMATION

Corresponding Authors

Haiteng Deng − *MOE Key Laboratory of Bioinformatics, Center for Synthetic and Systematic Biology, School of Life Sciences, Tsinghua University, Beijing 100084, P. R. China;* orcid.org/0000-0001-9496-1280; Email: dht@mail.tsinghua.edu.cn

Chongdong Liu − *Chao Yang Hospital of Capital Medical University, Beijing 100020, P. R. China;* Email: liuchongdong@ccmu.edu.cn

https://doi.org/10.1021/acsomega.2c04286
ACS Omega 2022, 7, 37509−37519

Authors

Changmei Yang − *MOE Key Laboratory of Bioinformatics, Center for Synthetic and Systematic Biology, School of Life Sciences, Tsinghua University, Beijing 100084, P. R. China*

Tianxiang Wang − *MOE Key Laboratory of Bioinformatics, Center for Synthetic and Systematic Biology, School of Life Sciences, Tsinghua University, Beijing 100084, P. R. China*

Songbiao Zhu − *MOE Key Laboratory of Bioinformatics, Center for Synthetic and Systematic Biology, School of Life Sciences, Tsinghua University, Beijing 100084, P. R. China*

Zhaoyun Zong − *MOE Key Laboratory of Bioinformatics, Center for Synthetic and Systematic Biology, School of Life Sciences, Tsinghua University, Beijing 100084, P. R. China*

Chengting Luo − *MOE Key Laboratory of Bioinformatics, Center for Synthetic and Systematic Biology, School of Life Sciences, Tsinghua University, Beijing 100084, P. R. China*

Yujiao Zhao − *MOE Key Laboratory of Bioinformatics, Center for Synthetic and Systematic Biology, School of Life Sciences, Tsinghua University, Beijing 100084, P. R. China*

Jing Liu − *MOE Key Laboratory of Bioinformatics, Center for Synthetic and Systematic Biology, School of Life Sciences, Tsinghua University, Beijing 100084, P. R. China*

Ting Li − *MOE Key Laboratory of Bioinformatics, Center for Synthetic and Systematic Biology, School of Life Sciences, Tsinghua University, Beijing 100084, P. R. China*

Xiaohui Liu − *MOE Key Laboratory of Bioinformatics, Center for Synthetic and Systematic Biology, School of Life Sciences, Tsinghua University, Beijing 100084, P. R. China*

Complete contact information is available at: https://pubs.acs.org/10.1021/acsomega.2c04286

Author Contributions

#C.Y. and T.W. contributed equally.

Author Contributions

H.D., C.Y., and T.W. designed research. C.Y. and T.W. did the experiments with help from S.Z., Z.Z., C.L., J.L., Y.Z., T.L., and C.L. C.Y. and H.D. wrote the manuscript. All authors reviewed, edited and approved the manuscript.

Notes

The authors declare no competing financial interest.

■ ACKNOWLEDGMENTS

This study was supported by the Ministry of Science and Technology of the People's Republic of China (Grant No. 2017YFA0505103 and No. 2020YFC2002705), and National Natural Science Foundation of China (Grant No. 21877068 and No. 20211300114). We greatly appreciate the Facility for Protein Chemistry and Proteomics at Tsinghua University for sample analysis.

■ ABBREVIATIONS

NNMT, nicotinamide *N*-methyltransferase
NAM, nicotinamide
1-MNAM, 1-methylnicotinamide
SAM, S-adenosyl-L-methionine
SAH, S-adenosyl-L-homocysteine
IL1β, interleukin 1β
COX2, cyclooxygenase-2
15-PGDH, 15-hydroxyprostaglandin dehydrogenase
PGE_2, prostaglandin E_2
CAFs, cancer-associated fibroblasts
HGSC, high-grade serous carcinoma
IARC, International Agency for Research on Cancer
NSCLC, nonsmall cell lung cancer
EMT, epithelial-mesenchymal transition
ROS, reactive oxygen species
NA, nicotinic acid
3-HK, 3-hydroxykynurenine
KYN, kynurenine
3-HAA, 3-hydroxyanthranilic acid
ECM, extracellular matrix
LC-MS/MS, liquid chromatography-tandem mass spectrometry
DDA, data-dependent acquisition
AGC, Automatic Gain Control
Trp, tryptophan
QA, quinolinic acid
PARPs, poly(ADP-ribose) polymerases
CD38, cluster of differentiation 38
GO, Gene Ontology
BP, biological processes
MF, molecular functions
CC, cellular component
IPA, Ingenuity Pathway Analysis
CHX, cycloheximide
IL11, interleukin 11
IL6, interleukin 6
MMP2, matrix metalloproteinase 2
VCAM1, vascular cell adhesion protein 1
TGM2, protein-glutamine gamma-glutamyltransferase 2
ADAM19, disintegrin and metalloproteinase domain-containing protein 19
CXCLs, C-X-C motif chemokines
TGFβ2, transforming growth factor β2
KP, kynurenine pathway
CEA, carcinoembryonic antigen
CRC, colorectal cancer

■ REFERENCES

(1) Sartini, D.; Morganti, S.; Guidi, E.; Rubini, C.; Zizzi, A.; Giuliante, R.; Pozzi, V.; Emanuelli, M. Nicotinamide N-methyltransferase in non-small cell lung cancer: promising results for targeted anti-cancer therapy. *Cell Biochem Biophys* **2013**, *67* (3), 865−73.

(2) Tang, Z.; Li, C.; Kang, B.; Gao, G.; Li, C.; Zhang, Z. GEPIA: a web server for cancer and normal gene expression profiling and interactive analyses. *Nucleic Acids Res.* **2017**, *45* (W1), W98−w102.

(3) Sartini, D.; Santarelli, A.; Rossi, V.; Goteri, G.; Rubini, C.; Ciavarella, D.; Lo Muzio, L.; Emanuelli, M. Nicotinamide N-methyltransferase upregulation inversely correlates with lymph node metastasis in oral squamous cell carcinoma. *Mol. Med. (Cambridge, Mass.)* **2007**, *13* (7−8), 415−21.

(4) Leal, M. F.; Chung, J.; Calcagno, D. Q.; Assumpção, P. P.; Demachki, S.; da Silva, I. D.; Chammas, R.; Burbano, R. R.; de Arruda Cardoso Smith, M. Differential proteomic analysis of noncardia gastric cancer from individuals of northern Brazil. *PLoS One* **2012**, *7* (7), e42255.

(5) Kanska, J.; Aspuria, P. P.; Taylor-Harding, B.; Spurka, L.; Funari, V.; Orsulic, S.; Karlan, B. Y.; Wiedemeyer, W. R. Glucose deprivation elicits phenotypic plasticity via ZEB1-mediated expression of NNMT. *Oncotarget* **2017**, *8* (16), 26200−26220.

(6) Eckert, M. A.; Coscia, F.; Chryplewicz, A.; Chang, J. W.; Hernandez, K. M.; Pan, S.; Tienda, S. M.; Nahotko, D. A.; Li, G.; Blaženović, I.; Lastra, R. R.; Curtis, M.; Yamada, S. D.; Perets, R.; McGregor, S. M.; Andrade, J.; Fiehn, O.; Moellering, R. E.; Mann, M.; Lengyel, E. Proteomics reveals NNMT as a master metabolic

https://doi.org/10.1021/acsomega.2c04286
ACS Omega 2022, 7, 37509−37519

regulator of cancer-associated fibroblasts. *Nature* **2019**, *569* (7758), 723−728.
(7) Sartini, D.; Seta, R.; Pozzi, V.; Morganti, S.; Rubini, C.; Zizzi, A.; Tomasetti, M.; Santarelli, L.; Emanuelli, M. Role of nicotinamide N-methyltransferase in non-small cell lung cancer: in vitro effect of shRNA-mediated gene silencing on tumourigenicity. *Biol. Chem.* **2015**, *396* (3), 225−34.
(8) Sung, H.; Ferlay, J.; Siegel, R. L.; Laversanne, M.; Soerjomataram, I.; Jemal, A.; Bray, F., Global cancer statistics 2020: GLOBOCAN estimates of incidence and mortality worldwide for 36 cancers in 185 countries. *CA* **2021**.
(9) Aisner, D. L.; Sholl, L. M.; Berry, L. D.; Rossi, M. R.; Chen, H.; Fujimoto, J.; Moreira, A. L.; Ramalingam, S. S.; Villaruz, L. C.; Otterson, G. A.; Haura, E.; Politi, K.; Glisson, B.; Cetnar, J.; Garon, E. B.; Schiller, J.; Waqar, S. N.; Sequist, L. V.; Brahmer, J.; Shyr, Y.; Kugler, K.; Wistuba, I. I.; Johnson, B. E.; Minna, J. D.; Kris, M. G.; Bunn, P. A.; Kwiatkowski, D. J. The Impact of Smoking and TP53 Mutations in Lung Adenocarcinoma Patients with Targetable Mutations-The Lung Cancer Mutation Consortium (LCMC2). *Clin. Cancer Res.* **2018**, *24* (5), 1038−1047.
(10) Gazdar, A. F.; Linnoila, R. I. The pathology of lung cancer–changing concepts and newer diagnostic techniques. *Semin Oncol* **1988**, *15* (3), 215−25.
(11) Tomida, M.; Ohtake, H.; Yokota, T.; Kobayashi, Y.; Kurosumi, M. Stat3 up-regulates expression of nicotinamide N-methyltransferase in human cancer cells. *J. Cancer Res. Clin Oncol* **2008**, *134* (5), 551−9.
(12) Tomida, M.; Mikami, I.; Takeuchi, S.; Nishimura, H.; Akiyama, H. Serum levels of nicotinamide N-methyltransferase in patients with lung cancer. *J. Cancer Res. Clin Oncol* **2009**, *135* (9), 1223−9.
(13) Bach, D. H.; Kim, D.; Bae, S. Y.; Kim, W. K.; Hong, J. Y.; Lee, H. J.; Rajasekaran, N.; Kwon, S.; Fan, Y.; Luu, T. T.; Shin, Y. K.; Lee, J.; Lee, S. K. Targeting Nicotinamide N-Methyltransferase and miR-449a in EGFR-TKI-Resistant Non-Small-Cell Lung Cancer Cells. *Mol. Ther Nucleic Acids* **2018**, *11*, 455−467.
(14) Pozzi, V.; Salvolini, E.; Lucarini, G.; Salvucci, A.; Campagna, R.; Rubini, C.; Sartini, D.; Emanuelli, M. Cancer stem cell enrichment is associated with enhancement of nicotinamide N-methyltransferase expression. *IUBMB life* **2020**, *72* (7), 1415−1425.
(15) Fang, E. F.; Lautrup, S.; Hou, Y.; Demarest, T. G.; Croteau, D. L.; Mattson, M. P.; Bohr, V. A. NAD(+) in Aging: Molecular Mechanisms and Translational Implications. *Trends Mol. Med.* **2017**, *23* (10), 899−916.
(16) Cantó, C.; Menzies, K. J.; Auwerx, J. NAD(+) Metabolism and the Control of Energy Homeostasis: A Balancing Act between Mitochondria and the Nucleus. *Cell Metab* **2015**, *22* (1), 31−53.
(17) Kraus, D.; Yang, Q.; Kong, D.; Banks, A. S.; Zhang, L.; Rodgers, J. T.; Pirinen, E.; Pulinilkunnil, T. C.; Gong, F.; Wang, Y. C.; Cen, Y.; Sauve, A. A.; Asara, J. M.; Peroni, O. D.; Monia, B. P.; Bhanot, S.; Alhonen, L.; Puigserver, P.; Kahn, B. B. Nicotinamide N-methyltransferase knockdown protects against diet-induced obesity. *Nature* **2014**, *508* (7495), 258−62.
(18) Xie, X.; Yu, H.; Wang, Y.; Zhou, Y.; Li, G.; Ruan, Z.; Li, F.; Wang, X.; Liu, H.; Zhang, J. Nicotinamide N-methyltransferase enhances the capacity of tumorigenesis associated with the promotion of cell cycle progression in human colorectal cancer cells. *Arch. Biochem. Biophys.* **2014**, *564*, 52−66.
(19) Wang, W.; Hu, Y.; Wang, X.; Wang, Q.; Deng, H. ROS-Mediated 15-Hydroxyprostaglandin Dehydrogenase Degradation via Cysteine Oxidation Promotes NAD(+)-Mediated Epithelial-Mesenchymal Transition. *Cell Chem. Biol.* **2018**, *25* (3), 255−261.e4.
(20) Wang, W.; Hu, Y.; Yang, C.; Zhu, S.; Wang, X.; Zhang, Z.; Deng, H. Decreased NAD Activates STAT3 and Integrin Pathways to Drive Epithelial-Mesenchymal Transition. *Mol. Cell Proteomics* **2018**, *17* (10), 2005−2017.
(21) Ulanovskaya, O. A.; Zuhl, A. M.; Cravatt, B. F. NNMT promotes epigenetic remodeling in cancer by creating a metabolic methylation sink. *Nat. Chem. Biol.* **2013**, *9* (5), 300−6.
(22) Yuan, M.; Breitkopf, S. B.; Yang, X.; Asara, J. M. A positive/negative ion-switching, targeted mass spectrometry-based metabolomics platform for bodily fluids, cells, and fresh and fixed tissue. *Nat. Protoc* **2012**, *7* (5), 872−81.
(23) Xu, J.; Zhu, S.; Xu, L.; Liu, X.; Ding, W.; Wang, Q.; Chen, Y.; Deng, H. CA9 Silencing Promotes Mitochondrial Biogenesis, Increases Putrescine Toxicity and Decreases Cell Motility to Suppress ccRCC Progression. *Int. J. Mol. Sci.* **2020**, *21* (16), 5939.
(24) Hu, Y.; Wang, H.; Wang, Q.; Deng, H. Overexpression of CD38 decreases cellular NAD levels and alters the expression of proteins involved in energy metabolism and antioxidant defense. *J. Proteome Res.* **2014**, *13* (2), 786−95.
(25) Darnell, J. E., Jr.; Kerr, I. M.; Stark, G. R. Jak-STAT pathways and transcriptional activation in response to IFNs and other extracellular signaling proteins. *Science (New York, N.Y.)* **1994**, *264* (5164), 1415−21.
(26) Ihle, J. N. Cytokine receptor signalling. *Nature* **1995**, *377* (6550), 591−4.
(27) Wang, R.; Cherukuri, P.; Luo, J. Activation of Stat3 sequence-specific DNA binding and transcription by p300/CREB-binding protein-mediated acetylation. *J. Biol. Chem.* **2005**, *280* (12), 11528−34.
(28) Yuan, Z. L.; Guan, Y. J.; Chatterjee, D.; Chin, Y. E. Stat3 dimerization regulated by reversible acetylation of a single lysine residue. *Science (New York, N.Y.)* **2005**, *307* (5707), 269−73.
(29) Yu, H.; Pardoll, D.; Jove, R. STATs in cancer inflammation and immunity: a leading role for STAT3. *Nat. Rev. Cancer* **2009**, *9* (11), 798−809.
(30) Zheng, C. C.; Hu, H. F.; Hong, P.; Zhang, Q. H.; Xu, W. W.; He, Q. Y.; Li, B. Significance of integrin-linked kinase (ILK) in tumorigenesis and its potential implication as a biomarker and therapeutic target for human cancer. *Am. J. Cancer Res.* **2019**, *9* (1), 186−197.
(31) Abrahao, A. C.; Castilho, R. M.; Squarize, C. H.; Molinolo, A. A.; dos Santos-Pinto, D., Jr.; Gutkind, J. S. A role for COX2-derived PGE2 and PGE2-receptor subtypes in head and neck squamous carcinoma cell proliferation. *Oral Oncol* **2010**, *46* (12), 880−7.
(32) Cipollone, F.; Cicolini, G.; Bucci, M. Cyclooxygenase and prostaglandin synthases in atherosclerosis: recent insights and future perspectives. *Pharmacol Ther* **2008**, *118* (2), 161−80.
(33) Baldan, A.; Ferronato, S.; Olivato, S.; Malerba, G.; Scuro, A.; Veraldi, G. F.; Gelati, M.; Ferrari, S.; Mariotto, S.; Pignatti, P. F.; Mazzucco, S.; Gomez-Lira, M. Cyclooxygenase 2, toll-like receptor 4 and interleukin 1β mRNA expression in atherosclerotic plaques of type 2 diabetic patients. *Inflamm Res.* **2014**, *63* (10), 851−8.
(34) Jaschinski, F.; Rothhammer, T.; Jachimczak, P.; Seitz, C.; Schneider, A.; Schlingensiepen, K. H. The antisense oligonucleotide trabedersen (AP 12009) for the targeted inhibition of TGF-β2. *Curr. Pharm. Biotechnol* **2011**, *12* (12), 2203−13.
(35) Mantovani, A.; Allavena, P.; Sica, A.; Balkwill, F. Cancer-related inflammation. *Nature* **2008**, *454* (7203), 436−44.
(36) Hsu, Y. C.; Chen, H. Y.; Yuan, S.; Yu, S. L.; Lin, C. H.; Wu, G.; Yang, P. C.; Li, K. C. Genome-wide analysis of three-way interplay among gene expression, cancer cell invasion and anti-cancer compound sensitivity. *BMC Med.* **2013**, *11*, 106.
(37) Lu, X. M.; Long, H. Nicotinamide N-methyltransferase as a potential marker for cancer. *Neoplasma* **2018**, *65* (5), 656−663.
(38) Wang, W.; Yang, C.; Wang, T.; Deng, H. Complex roles of nicotinamide N-methyltransferase in cancer progression. *Cell Death Dis* **2022**, *13* (3), 267.
(39) Mu, X.; Chen, Y.; Wang, S. H.; Li, M. The effect of nicotinamide N-methytransferase overexpression on biological behaviors of SMMC7721 hepatocellar carcinoma cell line. *Sichuan Da Xue Xue Bao Yi Xue Ban* **2013**, *44* (2), 193−5 and 217.
(40) Stefatić, D.; Riederer, M.; Balić, M.; Dandachi, N.; Stanzer, S.; Janesch, B.; Resel, M.; Ler, D.; Samonigg, H.; Bauernhofer, T. Optimization of diagnostic ELISA-based tests for the detection of auto-antibodies against tumor antigens in human serum. *Bosn J. Basic Med. Sci.* **2008**, *8* (3), 245−50.
(41) Li, T.; Le, A. Glutamine Metabolism in Cancer. *Adv. Exp. Med. Biol.* **2018**, *1063*, 13−32.

https://doi.org/10.1021/acsomega.2c04286
ACS Omega 2022, 7, 37509−37519

(42) Cluntun, A. A.; Lukey, M. J.; Cerione, R. A.; Locasale, J. W. Glutamine Metabolism in Cancer: Understanding the Heterogeneity. *Trends Cancer* **2017**, *3* (3), 169−180.
(43) Heng, B.; Lim, C. K.; Lovejoy, D. B.; Bessede, A.; Gluch, L.; Guillemin, G. J. Understanding the role of the kynurenine pathway in human breast cancer immunobiology. *Oncotarget* **2016**, *7* (6), 6506−20.
(44) Karayama, M.; Masuda, J.; Mori, K.; Yasui, H.; Hozumi, H.; Suzuki, Y.; Furuhashi, K.; Fujisawa, T.; Enomoto, N.; Nakamura, Y.; Inui, N.; Suda, T.; Maekawa, M.; Sugimura, H.; Takada, A. Comprehensive assessment of multiple tryptophan metabolites as potential biomarkers for immune checkpoint inhibitors in patients with non-small cell lung cancer. *Clin Transl Oncol* **2021**, *23* (2), 418−423.
(45) Tong, M.; Ding, Y.; Tai, H. H. Reciprocal regulation of cyclooxygenase-2 and 15-hydroxyprostaglandin dehydrogenase expression in A549 human lung adenocarcinoma cells. *Carcinogenesis* **2006**, *27* (11), 2170−9.
(46) Che, D.; Zhang, S.; Jing, Z.; Shang, L.; Jin, S.; Liu, F.; Shen, J.; Li, Y.; Hu, J.; Meng, Q.; Yu, Y. Macrophages induce EMT to promote invasion of lung cancer cells through the IL-6-mediated COX-2/PGE(2)/β-catenin signalling pathway. *Mol. Immunol* **2017**, *90*, 197−210.
(47) Jiang, G. B.; Fang, H. Y.; Tao, D. Y.; Chen, X. P.; Cao, F. L. COX-2 potentiates cisplatin resistance of non-small cell lung cancer cells by promoting EMT in an AKT signaling pathway-dependent manner. *Eur. Rev. Med. Pharmacol Sci.* **2019**, *23* (9), 3838−3846.

https://doi.org/10.1021/acsomega.2c04286
ACS Omega 2022, 7, 37509−37519